INDONESIAN JOURNAL ON GEOSCIENCE
Geological Agency
Ministry of Energy and Mineral Resources

Journal homepage: https://ijog.geologi.esdm.go.id
ISSN 2355-9314, e-ISSN 2355-9306

Makassar Strait Thrust - Mamuju Segment (MSTM) Perspective on Radioactive Mineral Exploration: A Case Study in Rantedoda, Mamuju

Roni Cahya Ciputra[1], Fadiah Pratiwi[1], Aldo Febriansyah Putra[2], Heri Syaeful[1], Frederikus Dian Indrastomo[1], Tyto Baskara Adimedha[1], Yoshi Rachael[1], and I Gde Sukadana[1]

[1]Research Center for Nuclear Material and Radioactive Waste Technology, National Research and Innovation Agency (BRIN), Tangerang Selatan 15314, Indonesia
[2]Department of Geosciences, Faculty of Mathematics and Natural Sciences, Universitas Indonesia, Depok 16424, Indonesia

Corresponding Author: roni010@brin.go.id
Manuscript received: December, 23, 2024; revised: March, 04, 2025;
approved: August, 11, 2025; available online: September, 24, 2025

Abstract - The Makassar Strait Thrust – Mamuju Segment (MSTM) is a key structural feature influencing uranium (U), thorium (Th), and rare earth element (REE) mineralization in Mamuju, West Sulawesi. This study explores a relationship between tectonic deformation, weathering processes, and mineralization, focusing on the Rantedoda sector. Integrated geomorphic, geological, radiometric, petrographic, and geochemical analyses reveal that MSTM faults act as conduits for hydrothermal fluids, promoting mineral mobilization, alteration, and enrichment in fault zones. MSTM produced curved NW−SE to N−S thrusts torn by NE−SW right-lateral strike-slip faults in the studied area. Radiometric data highlight anisotropic distributions of U, Th, and dose rates aligned with NE−SW and NW−SE fault trends. Geochemical indices demonstrate that weathering is critical for REE and Th enrichment, as high eTh and low K values indicate. Moreover, fault-facilitated hydrothermal clay alteration supports U adsorption, as noted by high values of all radiometric parameters in the area near a fault. These findings establish the critical role of fault systems in controlling mineralization processes, providing a framework for targeted exploration strategies in tectonically complex terrains of the Mamuju area.

Keywords: Mamuju, Rantedoda, uranium, thorium, REE, Makassar Strait Thrust, Faults

How to cite this article:
Ciputra, R.C., Pratiwi, F., Putra, A.F., Syaeful, H., Indrastomo, F.D., Adimedha, T.B., Rachael, Y., and Sukadana, I.G., 2025. Makassar Strait Thrust - Mamuju Segment (MSTM) Perspective on Radioactive Mineral Exploration: A Case Study in Rantedoda, Mamuju. *Indonesian Journal on Geoscience*, 12 (3), p.319-341. DOI: 10.17014/ijog.12.3.319-341

Introduction

Background

Nuclear energy is encouraged to be one of Indonesia programmes to fulfill its commitment to Net Zero Emission (NZE) by 2060 (Permana *et al.*, 2022; Kanugrahan and Hakam, 2023; Shah *et al.*, 2024). Nuclear Power Plant (NPP) implementation in the Indonesian electricity system simulation showed that NPP could significantly satisfy the nation electrical energy needs while simultaneously reducing CO_2 emissions, given the limited implementation of other low-carbon, renewable energy sources like hydro, geothermal, solar, and wind power (Rahmanta *et al.*, 2023). Other simulations noted that NPP would contribute the most to the nation energy share among all renewable energy sources (Permana *et al.*, 2022). Those findings on the importance of NPP deployment also imply the importance of nuclear energy

system development, including the development of the raw nuclear materials that will emerge as strategic commodities.

Indonesia's raw nuclear materials are available from uranium and thorium deposits in Kalimantan, Sulawesi, Sumatra, Papua, Bangka-Belitung, and the Riau Islands (Syaeful *et al.*, 2021). Particularly in Sulawesi, the Mamuju area of West Sulawesi has volcanogenic-type deposits in the Adang Volcanic Rocks (Mu'awanah *et al.*, 2019; Rosianna *et al.*, 2020, 2023; Sukadana *et al.*, 2015, 2021). The Adang Volcanic Rock magma is highly alkaline, ranging from sodic to ultrapotassic. It has a diverse magma series, including tholeiitic, calc-alkali, high-K calc-alkali, and shoshonite magmas. Based on geochemical data, the rocks are basaltic trachyandesite, trachyandesite, andesite, tephriphonolite, and trachyte (Syaeful *et al.*, 2014).

Highly naturally occurring radioactive materials (NORM) have been identified coming from The Adang Volcanic Rock, contributing to Mamuju highest average dose rate in Sulawesi and even Indonesian regions, which can reach 2,800 nSv/h, (Syaeful *et al.*, 2014). The isotope characterization reveals the ^{238}U and ^{232}Th concentrations of laterite and rock of the area to be 22,882 and 33,549 Bq/kg on average (Rosianna *et al.*, 2023). The Rosianna *et al.* (2023) study also shows that equilibrium uranium is further remobilized, interpreted as influenced by groundwater and the reduction-oxidation environment. There are two types of uranium and thorium mineralization in Mamuju: volcanic and lateritic deposits. The volcanic deposit can be distinguished into strata-bound and structure-bound deposits (Sukadana *et al.*, 2016; Rosianna *et al.*, 2023; Syaeful *et al.*, 2024). The primary radioactive minerals identified in Mamuju are davidite and thorianite, while the secondary minerals are gummite and autunite. SEM-EDS Point analysis in thorianite mineral shows 1.16 wt. % and 31.14 wt. % for uranium and thorium, respectively (Sukadana *et al.*, 2016). Investigation in weathered volcanic rock in Mamuju area showed a strong indication of the REE-rich mineral of zircon with values ranging from 567 -6400 ppm in the weathering profile of the phonolitic leucitite rock, specifically in Kelapa Tujuh and North Botteng Villages (Ritonga *et al.*, 2021). The Geochemical analysis on veins in Hulu Mamuju area shows several Th and REE-bearing minerals of britholite, aeschynite, monazite, chevkinite-Ce, thorite, and thorutite (Sukadana *et al.*, 2022). The samples are altered, and Th content is elevated to 7.4 %, while total REE content is elevated to 4.8 %. Radiometric analysis also shows enrichment of Th in the altered and weathered region of Adang Volcanic Rocks in Mamuju (Syaeful *et al.*, 2014; Sukadana *et al.*, 2021). Adang Volcanic Rock is among the rock formations affected by the presence of The Makassar Strait Thrust (MST) in the west (Guntoro, 1999; Puspita *et al.*, 2005).

The MST segment west of Mamuju is The Makassar Strait Thrust Mamuju Segment (MSTM) (Meilano *et al.*, 2023; Serhalawan and Chen, 2024). The MST is active and contributes to the higher crustal strain rate of Mamuju and Majene relative to their surrounding areas, causing a damaging earthquake in 2021 (Meilano *et al.*, 2023). A remote sensing analysis indicated that the SE–NW lineament system in Mamuju controlled volcano distribution and U-Th mineralization based on their similar distribution (Indrastomo *et al.*, 2017), yet how the identified lineament system influences the mineralization remains unclear. The MSTM contribution to uranium mineralization in Mamuju needs to be discussed to address any implications for the exploration programme. This work covers that topic by integrating geology, geophysics, and geochemistry of a sector in Mamuju as a case study to fill the gap in research. Rantedoda Sector is one of the areas with the radiometric anomaly in Mamuju (Sukadana *et al.*, 2021). A further study reveals higher U content of samples from this sector up to 0.09 wt. % UO_2, 0.13 wt. % ThO_2, and 1.21 wt. % total REE content (Pratiwi *et al.*, 2024). This sector was chosen for the case study, because it had high levels of U, Th, and REE in a region affected by MSTM activity that led to the formation of a thrust belt known as The Mamuju Thrust Belt (MTB), characterized by numerous structural features.

Geological Settings

The tectonic setting of Sulawesi is built by the interactions among three major plates: the

Eurasian Continental Plate, the Oceanic-Continental Indo-Australian Plate, and the Oceanic Pacific-Philippine Sea Plate. Tectonic events from the Late Mesozoic to the Cenozoic created four tectonic provinces, namely The Western-Northern Sulawesi Magmatic Arc (comprising south, west, neck, and north arms), The Central Sulawesi Metamorphic Belt, The East Sulawesi Ophiolite (east arm), and The Banggai-Sula and Buton-Tukangbesi Microcontinental Fragments (Maulana *et al.*, 2016). This study is located in West Sulawesi region, as illustrated by Figure 1a, which is currently developed as a fold-thrust belt with active seismicity (Meilano *et al*., 2023).

The tectonic evolution of West Sulawesi region began in the Late Cretaceous when the East Java-West Sulawesi Block was accreted to the margin of Sundaland (Hall and Sevast-

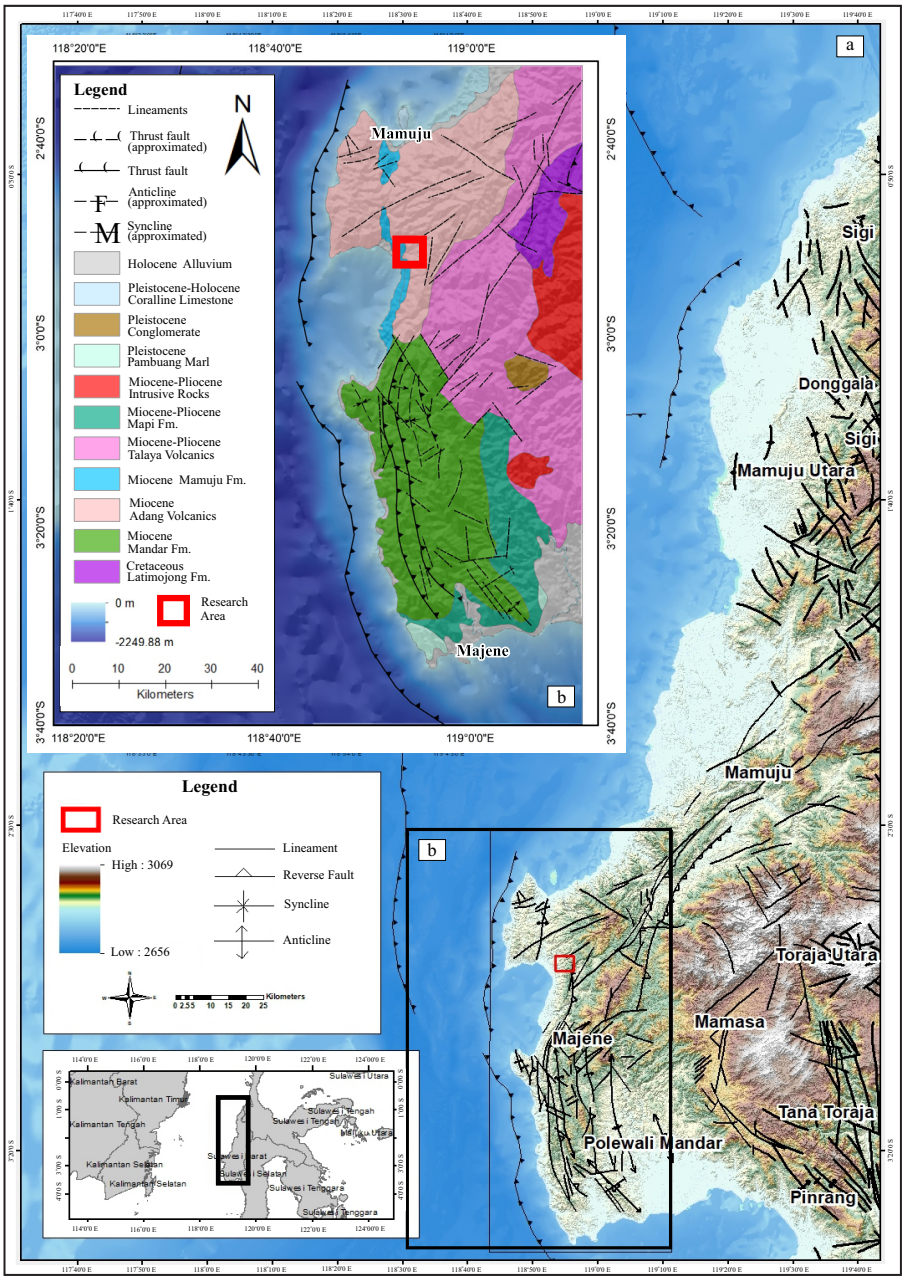

Figure 1. (a) Regional structural map of the West Sulawesi region (northern part: about 0°50'0°S to 2°30'0°S; southern part: approximately 2°30'0°S to 3°30'0°S) and (b) Geologic map of the southern part of the West Sulawesi region. The maps are modified after Bachri and Baharuddin (2001), Calvert and Hall (2007), Coffield *et al.* (1993), Ratman and Atmawinata (1993).

janova, 2012). A west-dipping subduction zone then developed east of the West Sulawesi region (*e.g*. Moss and Chambers, 1999; Elburg *et al*., 2003; Hall and Sevastjanova, 2012). The roll-back of this subduction zone caused the rifting of Makassar Strait Basin, and West Sulawesi region moved away from Kalimantan starting in Early Eocene (Simandjuntak, 1986; Guntoro, 1999; Hall and Sevastjanova, 2012). From the Middle to Late Eocene, the West Sulawesi region underwent a syn-rift phase that included terrestrial, transitional, and marine environments. The marine post-rift phase began in Oligocene (Coffield *et al.*, 1993; Calvert and Hall, 2007). The subduction-related magmatism in the West Sulawesi Region stretched from Paleocene to Early Miocene (*e.g*. Polvé *et al*., 1997; Elburg *et al.*, 2003; Leeuwen and Muhardjo, 2005). Extension-related magmatism developed from Middle Miocene to Late Pliocene (Elburg *et al.*, 2003; Hennig *et al.*, 2016). During Pliocene, the extension-related magmatism developed simultaneously with metamorphism (Hennig *et al.*, 2017). The West Sulawesi region underwent a major tectonic uplift in Plio-Pleistocene by the formation of the fold-thrust belt (Coffield *et al.*, 1993; Leeuwen and Muhardjo, 2005; Calvert and Hall, 2007).

Present-day structural features of the West Sulawesi region, as shown in Figure 1a, are inverted half-graben and fold-thrust belts that developed due to the Plio-Pleistocene compressional deformation (Coffield *et al.*, 1993; Leeuwen and Muhardjo, 2005; Puspita *et al.*, 2005; Calvert and Hall, 2007; Raharjo *et al.*, 2012). In the northern part of the region, the NE-SW half-graben system and NW-SE transfer faults were subjected to inversion (Calvert and Hall, 2007; Raharjo *et al.*, 2012). Folds in the area are trending in the N-S direction, and the mountain fronts in the northern part of the region are thrust-related (Calvert and Hall, 2007). The fold-thrust belt in the southern part of the region, as depicted by Figures 1a and 1b, changed its trend into an N−S direction, and it showed imbricating geometry (Coffield *et al.*, 1993). The 2021 Mw 6.2 earthquake in Mamuju showed that the southern part of the region was related to thrusting along the east-dipping fault plane (Meilano *et al.*, 2023).

Stratigraphy of the Mamuju area is composed of a distribution of volcanic rocks and marine sedimentary rocks (Ratman and Atmawinata, 1993). The constituent rocks of this area from the oldest are Middle Miocene - Pliocene Talaya Volcanic Rocks, Middle Miocene - Late Miocene Adang Volcanic Rocks, Middle Miocene - Late Miocene Mamuju Formation limestone with its Late Miocene Tapalang Member limestone, and Holocene coral limestone and alluvial deposits. The Adang Volcanic Rock comprises trachyte-phonolite rocks with ultrapotassic magmatic affinity from an Active Continental Margin (Sukadana *et al.*, 2015). The Adang Volcanic Rock also can be divided into several volcanostratigraphic units based on their volcanic features (Indrastomo *et al.*, 2015; Sukadana *et al.*, 2015; Sukadana, 2023), as shown in Figure 2. The researched area is Rantedoda Lava, Takandeang Lava, and Limestone units.

Methods

In this research, a geomorphic analysis desk study was done using a NASA Digital Elevation Model (NASADEM) image to identify the structural features of the area, and to guide the fieldwork. The NASADEM was created from the Shuttle Radar Topographic Mission (SRTM) reprocessing (Crippen *et al.*, 2016). In generating NASADEM, the vertical control of SRTM was improved with ICESat (Ice, Cloud, and Land Elevation Satellite) elevations, a precise elevation gained from laser altimetry techniques. The voids on the predecessor were filled with The Advanced Spaceborne Thermal Emission and Reflection Radiometer Global Digital Elevation Model (ASTER GDEM) (Crippen *et al.*, 2016). The geomorphic analysis was conducted by observing the geomorphic expressions size, shape, arrangement, and textures. This observation led to identifying landform types and lineaments and, thus, to interpreting structural features.

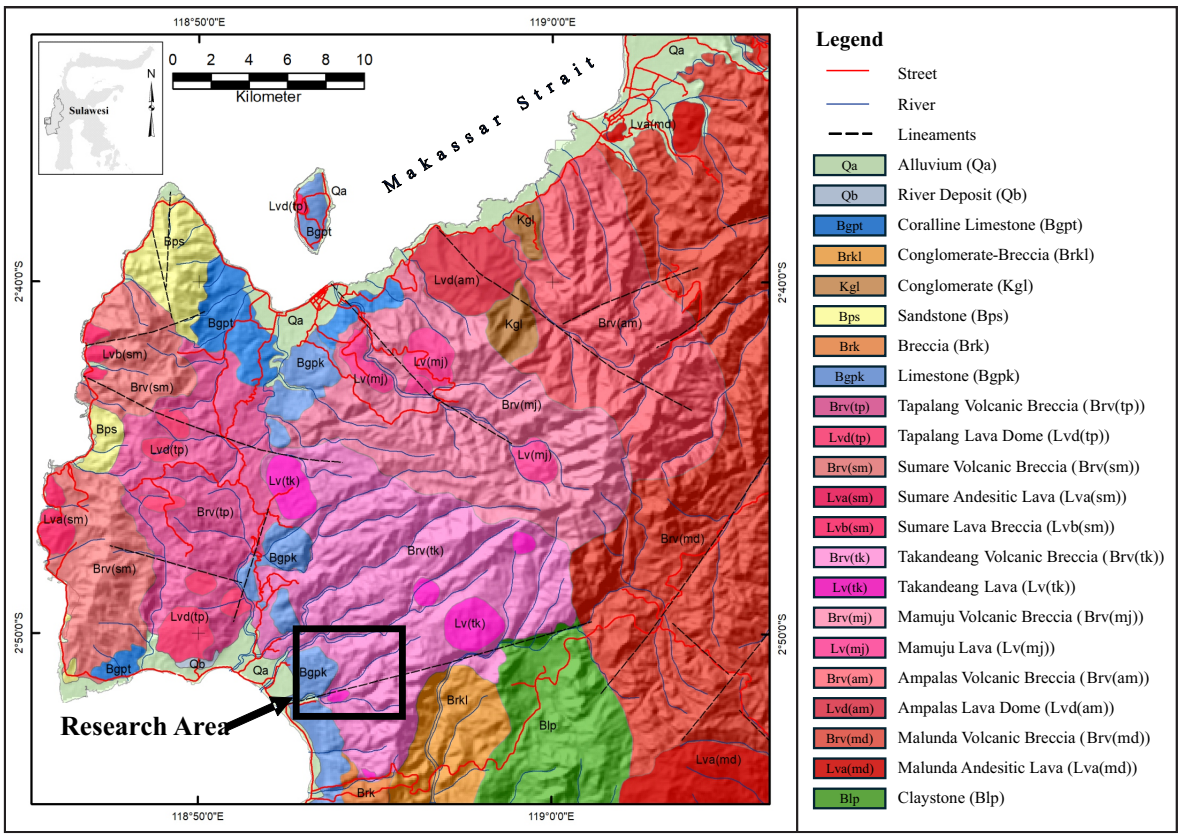

Figure 2. Geological Map of Mamuju area [modified from Rosianna *et al.* (2023) and Sukadana (2023)].

The fieldwork comprised (1) geological observation and mapping to obtain lithology and structural geology data, (2) rock and soil sampling for geochemical analysis and petrographic analysis of the rock samples, and (3) radiometric mapping for videography and anisotropy analysis of the radionuclides. A structural geological analysis of the fieldwork was done to confirm the geomorphic analysis. Fault slip data were collected and analyzed using the open-source WinTensor (Delvaux and Sperner, 2003) downloaded from https://damiendelvaux.be/Tensor/WinTensor/win-tensor.html to determine the fault's type and kinematics.

Rock samples were taken from a chip sampling using a geological hammer and a portable hand drill. Meanwhile, soil samples were obtained from the soil strata above the bedrock, free of plant organic components. The geochemical analysis was performed with Energy Disperse X-ray Fluorescence (ED XRF) Spectro XEPOS in the BRIN laboratory for twenty-five rock samples and fourteen soil samples representing different lithologies. Geochemical analysis for major elements using the XRF method has been conducted by several researchers in geochemistry within the exploration of rare earth mineral deposits (Hartiningsih *et al.*, 2022; Odigo *et al.*, 2023; and Winarno *et al.*, 2023). Eight samples were for petrographic analysis with the same representation purpose as the geochemical analysis.

Several indices were used to infer the rock weathering degrees: Lost on Ignition (LOI), Chemical Index of Alteration (CIA), and Index of Lateritization (IOL). These indices are calculated based on major element concentration in the weathered products. Chemical Index of Alteration (CIA), noted as (1), was used to evaluate the formation of clay minerals from feldspars.

$$\mathrm{CIA} = [Al_2O_3/(Al_2O_3 + CaO + Na_2O + K_2O)] \times 100 \quad ...(1)$$

where oxides are expressed in molar proportions.

Index of Lateritization (IOL), expressed as (2), measured the degree of lateritization in extreme weathering conditions, which CIA cannot accurately measure.

$$IOL = [(Al_2O_3 + Fe_2O_3)/(Al_2O_3 + Fe_2O_3 + SiO_2)] \times 100 \quad ...(2)$$

The radiometric mapping was retrieved from a GPS-linked RS-125 gamma spectrometer carried by the moving person and measured the concentration of radionuclides in 1-minute intervals. The variography and anisotropy analysis of the radiometric data was done using ArcGIS, followed by kriging interpolation to make radionuclides distribution maps. All the data were then synthesized to identify the relation between the MSTM-contributed structural features of Rantedoda to the U, Th, and REE enrichment and their implication on the exploration strategies.

Result

Geomorphic And Fault Slip Analyses

The studied area shows mountainous and low-relief terrains separated by thrust-related mountain fronts (Figure 3a). The elevation ranges from sea level to 888 m. The mountainous terrains show rugged and mottled topographic features (Figure 3a), as the former is underlain by Takandeang Volcanic Breccia and Takandeang Lava, while the latter is underlain by limestone (see Figure 2). The smooth, low-relief terrains correspond to alluvial (see Figure 2). The main structural features of the thrust-related mountain fronts are curved NW–SE to N–S thrusts torn by NE–SW right-lateral strike-slip faults (Figure 3a). The NE−SW right-lateral strike-slip faults (S1, S2, and S3) accommodate changes in the trend of the NW–SE to N–S thrust faults (T1, T2, and T3). Thrust occurring in this studied area displays imbricating geometry. The T1 and T2 Thrusts are the main faults, while the others occur as backthrusts. The T1 and T2 Thrusts form the mountain fronts, and the backthrusts are expressed as thrust valleys (Figures 3a to 3c). On the other hand, the right-lateral strike-slip faults are arranged subparallel to each other. Geomorphic expressions of the strike-slip faults are fault ridges (The S3 Fault) and linear fault valleys (The S1, S2, S4, and S5 Faults). Due to the heavily weathered outcrops, limited fault planes are preserved for structural analysis. However, field structural data acquired in the S4 Fault (a and b stations of Figure 3a) show NE−SW right-lateral strike-slip faults formed due to WNW–ESE compression (Figures 4a and 4b). Hot springs are found in a river and slopes. They are found near the S1 and T3 Faults and are interpreted to be related to the faults. The example of a hot spring located in the c station of Figure 3a is depicted in Figure 4c.

Stratigraphy

Geological observations resulted in the distribution of rock units in the researched area being divided into four units: Tasipa Lava, Rantedoda Lava, Sandstone, and Limestone. Rock and soil sampling was performed in Tasipa and Rantedoda Lavas, the host rock of volcanogenic-type mineralization. The geological map and sample distribution are displayed in Figure 5.

Tasipa lava appearance in the field is generally fresh, while the altered outcrops are found in the north and northeast. The example of the Tasipa lava outcrop is depicted in Figure 6a. It is a porphyro-aphanitic foiditoid rock with phenocrysts that include leucite, biotite, pyroxene, and hornblende (Figure 6b). The Rantedoda Lava has several dome features, as observed from the circular features in the DEM (Figure 5). These units have flowing structures, auto breccia, and sheeting joints (Figure 6c). It also consists of foiditoid rocks with a mineral composition of leucite, biotite, and pyroxene. It has a porphyro-afhanitic to porphyro-phaneritic texture (Figure 6d). However, it has a relatively smaller phenocryst than the Tasipa Lava.

The Sandstone Unit consists of sandstone, claystone, conglomerate, and coal are found around the valley in the northwest and southwest. The boulders of the conglomerate measuring 5 - 30 cm with closed packs were discovered at this location (Figure 6e). Contact outcrops between the Tasipa Lava unit and the conglomerate layers are found in the studied location, northern part of the studied

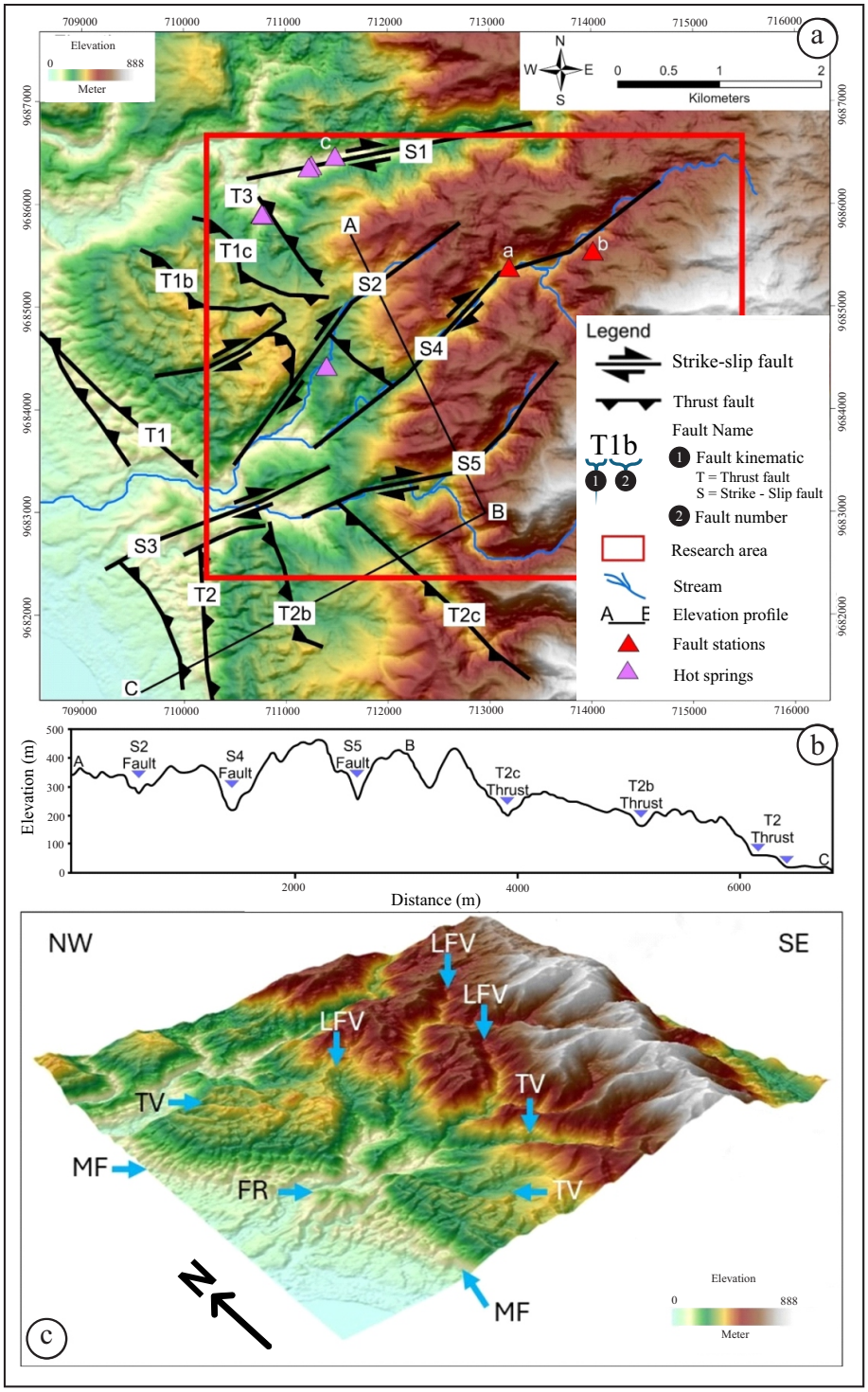

Figure 3. (a) Structural map, (b) Elevation profile, (c) Three-dimensional view of the studied area (MF: mountain front; TV: thrust valley; FR: fault ridge; LFV: linear fault valley).

area (Figure 6f). Layers of grey sandstone with fossilized shell material as a matrix were found on claystone layers found predominantly at the studied site, as examples in Figure 6g. Coal seams were also found at two locations southwest of the researched location on the Rantedoda branch of the river. At least two locations of coal outcrops were found in the river fork (Figure 6h). The limestone unit found in the southwestern part of the studied site is close to the morphology of the lowlands in

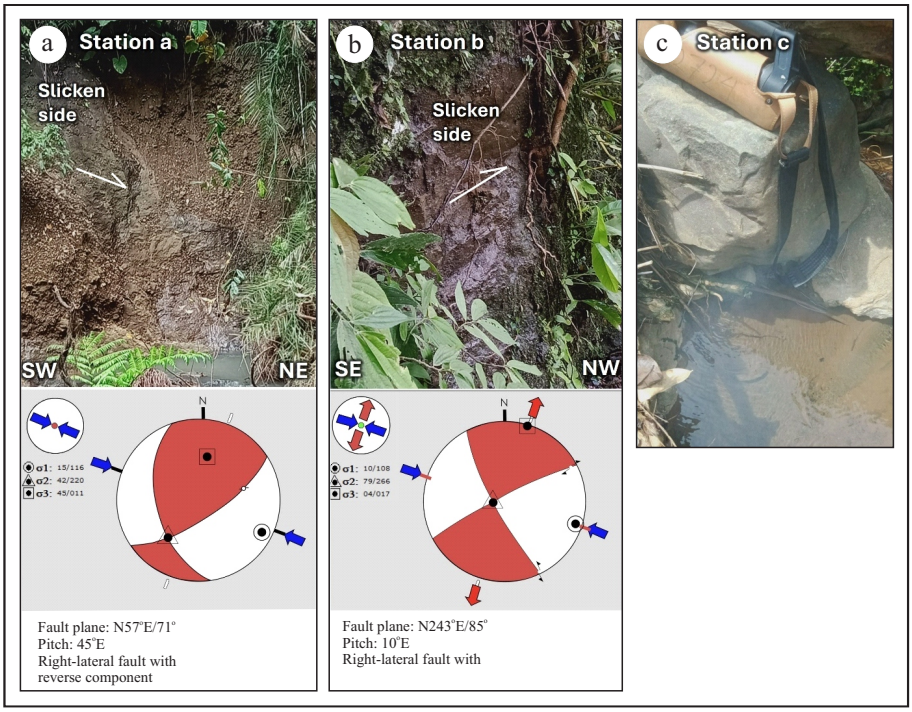

Figure 4. (a) Fault-slip analysis of the S4 Fault on station a; (b) Fault-slip analysis of the S4 Fault on station b; and (c) Spring on the river along the S1 Fault.

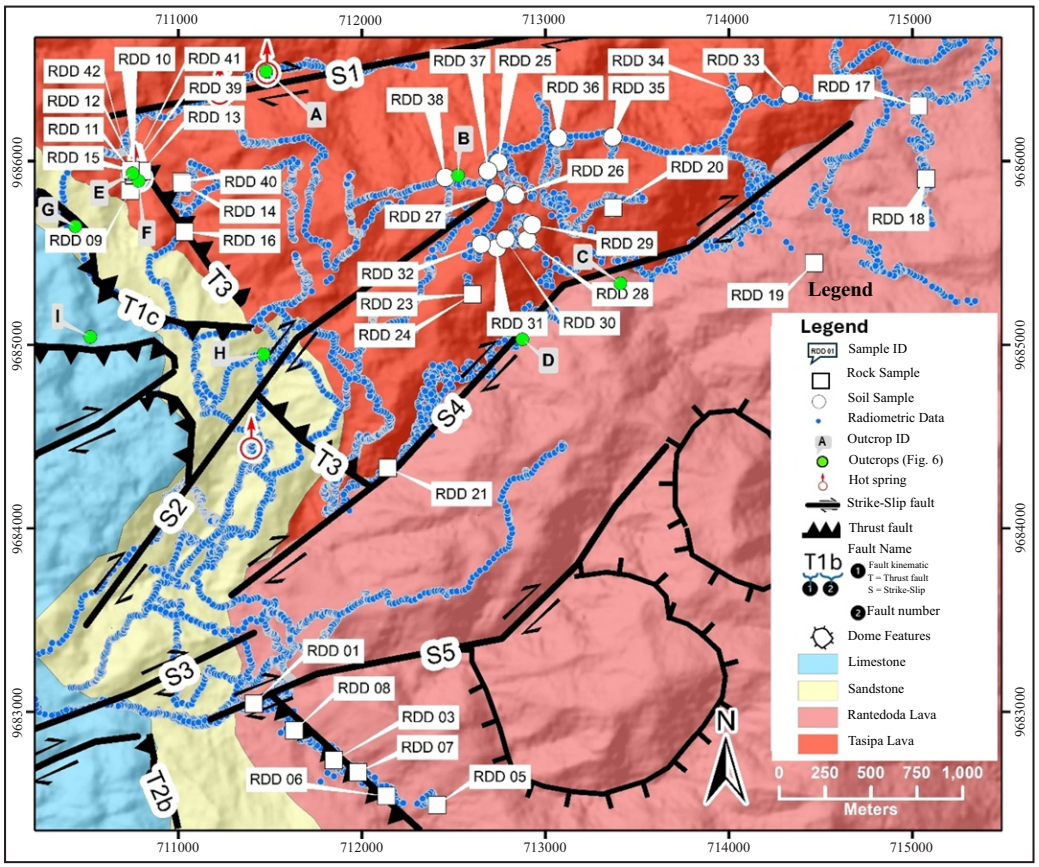

Figure 5. Geological map overlayed with radiometric data and sample distribution.

Figure 6. (a) Tasipa lava outcrop; (b) Tasipa lava megascopic appearance; (c) Rantedoda lava megascopic appeareance; (d) Rantedoda lava outcrop showing sheeting joints; (e) Basal conglomerate of Sandstone Unit; (f) Contact between conglomerate and lava; (g) Layers of sandstone and claystone of Sandstone Unit; and (h) Coal seam layer outcrop of Sandstone Unit; (i) Limestone outcrop above lava; location of these outcrops is depicted in Figure 5

Rantedoda Village. The unit consists of reef and clastic limestone that grow on the claystone and Tasipa Lava (Figure 6i). The limestone has been undergoing a diagenetic process at several places that producing crystalline limestone.

Petrographic Analysis

Among eight volcanic rock samples, four samples were taken from Rantedoda Lava Unit (RDD 17, RDD 18, RDD 5, and RDD 1), and four samples were from Tasipa Lava Unit (RDD 9, RDD 12, RDD 15, and RDD 41). Based on petrography observation, the general mineralogy of all the samples is closely identical. The phenocryst and groundmass predominantly are feldspathoid minerals such as leucite, pyroxene, biotite, alkali feldspar, and volcanic glass. Volcanic rocks from the researched area do not have any quartz content, which indicates that these rocks have a low level of silica saturation. Based on mineral composition, all the volcanic rocks in Rantedoda are Foidit (Table 1). Some examples of the photomicrograph showing petrographic textures of the sample can be seen in Figure 7.

The rock samples show porphyritic texture, with a skeletal texture very common in leucite mineral groundmass. Porphyritic texture indicates at least two crystallization processes: phenocryst crystallization occurs first, producing larger minerals, and then the groundmass crystallization process produces finer minerals. Skeletal texture indicates the crystal mineral develops under

Table 1. Mineralogical Composition of Lava Rock from Rantedoda Area

Code	Phenocryst Composition (%)				Groundmass Composition (%)			Lithology
	Leu	Px	Alf	Bt	Leu	Px needles	Glass	
RDD 17	5	5	-	-	85	5	-	Foidit
RDD 18	3	3	-	10	75	10	-	Foidit
RDD 1	10	5	-	-	75	10	-	Foidit
RDD 5	5	5	3	3	50	34	-	Foidit
RDD 9	35	20	5	5	10	-	25	Foidit
RDD 12	25	15	-	-	45	15	-	Foidit
RDD 15	35	20	5	-	20	-	20	Foidit
RDD 41	5	5	-	-	45	35	10	Foidit

Leu: Leucite, Px: Pyroxene, Alf: Alkali Feldspar, Bt: Biotite

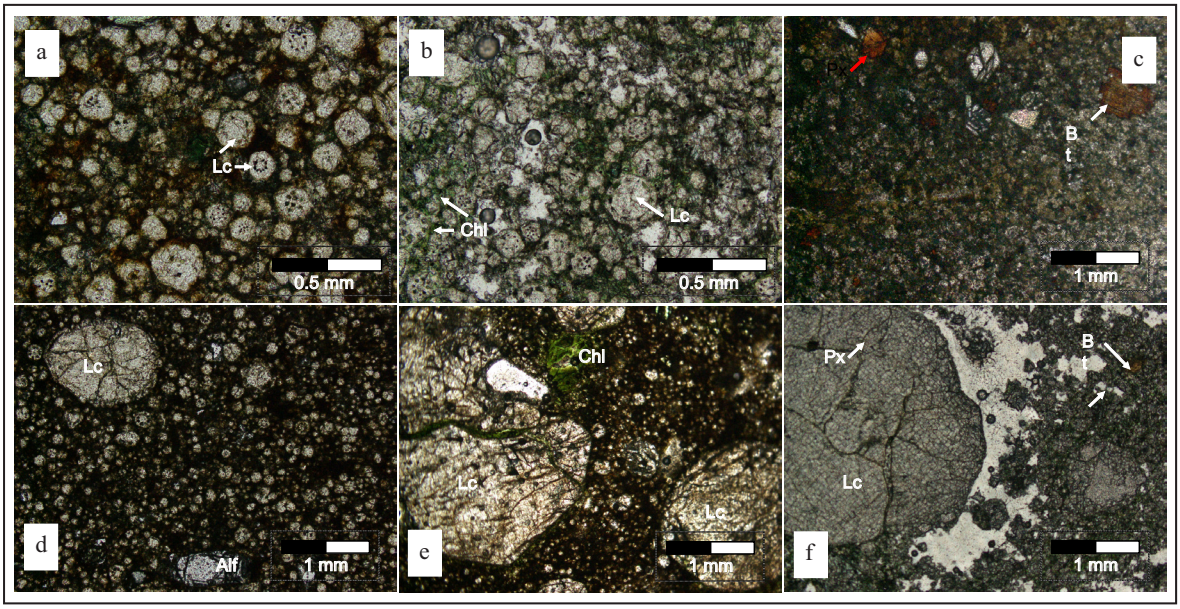

Figure 7. Skeletal texture observed in leucite mineral from (a) RDD 1 and (b) RDD 12, (c) and (d) Photomicrograph of foidit lava from Rantedoda Unit, (e) and (f) Photomicrograph of foidit lava from Tasipa Unit. Abbreviation: Lc: leucite, px: pyroxene, bt: biotite, alf: alkali feldspar, chl: chlorite.

conditions of rapid growth and a high degree of supersaturation. The difference between Tasipa Lava Unit and Rantedoda LavaUunit can be seen from the size of the phenocryst, percentage, and the composition of the groundmass. The Tasipa Lava Unit has bigger phenocrysts and more phenocryst content than the Rantedoda Lava Unit, and the presence of glass groundmass in the Tasipa Lava Unit also differentiates it from the Rantedoda Lava Unit. Some of the samples show evidence of weathering/alteration, clay masses (brown-black in thin sections) are observed in the groundmass of the samples (*e.g.* in RDD 17, 18, 1, 5, 9, and 15), zeolite is observed growing in vesicles (*e.g.* in RDD 15 and 41), and chlorite is observed in groundmass and fracture of minerals (*e.g.* in RDD 1, 12, and 15). Calcite was found growing in fracture (*e.g.* in RDD 15).

Geochemistry

About thirty-nine rock and soil samples from different units were collected. Major and trace element measurements were done using X-ray fluorescence. The XRF result for rock samples from the studied location has a SiO_2 content range from 44.09 - 60.27 wt. %, which means the rocks belong to the basaltic–intermediate group. The results from various diagrams are shown below to classify the Rantedoda and Tasipa Lava groups, and to explain their tectonic environment. Based

on Winchester and Floyd (1977) rocks samples from Rantedoda Lava and Tasipa Lava belong to basanite-trachybasanite, phonolite, and trachyandesite (Figure 8a), with magma affinity range from calc-alkaline series to shosonitic series (Peccerillo and Taylor, 1976) (Figure 8b). Rantedoda and Tasipa Lava groups show high alkalinity, ranging from calc-alkaline to shosonitic. Rocks with high alkalinity are usually found in tectonic settings related to continental crust, further away from the trench, and rarely in early subduction processes (Pearce and Cann, 1973; Winter, 2014).

Tectonic setting determination using Th-Zr/117-Nb/16 diagram, depicted in Figure 9a (Wood, 1980), suggest that both Rantedoda and Tasipa Lava groups was formed in the Arc Basalt Environment. On Zr/Y vs Zr diagram, displayed in Figure 9b (Pearce, 1983), both of the groups

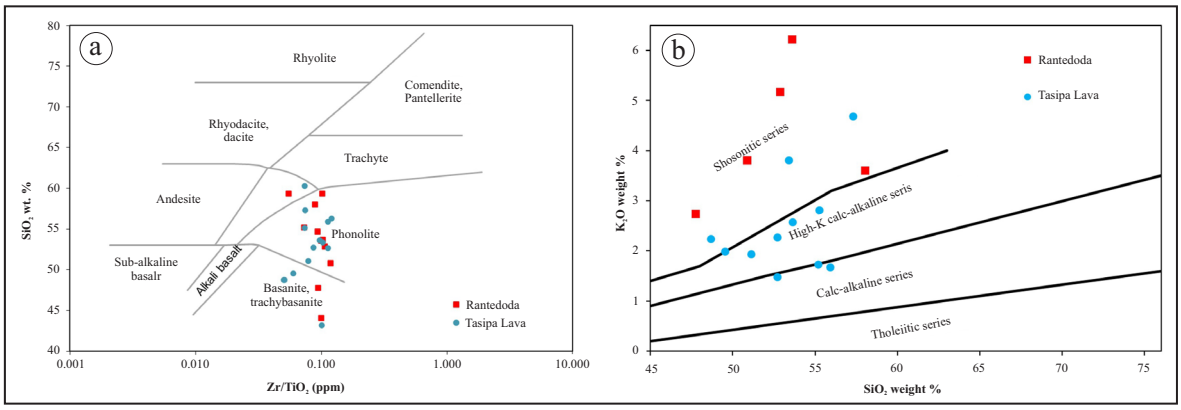

Figure 8. (a) Zr/TiO_2 vs SiO_2 diagram and (b) SiO_2 vs K_2O diagram.

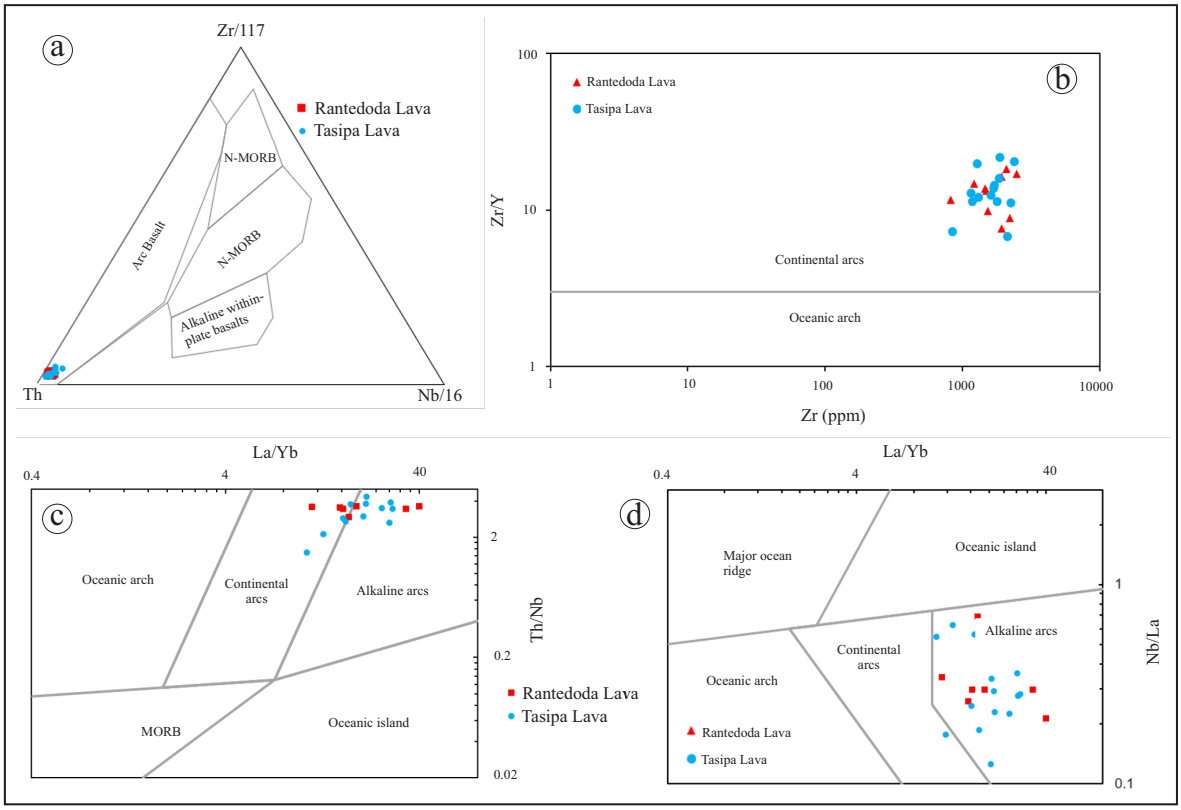

Figure 9. Tectonic setting discriminant diagram: (a) Th-Zr/117-Nb/16 diagram (Wood, 1980); (b) Zr/Y vs Zr diagram (Pearce, 1983); (c) La/Yb vs Nb/La and (d) La/Yb vs Th/Nb diagrams (Kurt Hollocher *et al*., 2012)

plotted on Continental Arcs. La/Yb vs Nb/La and La/Yb vs Th/Nb diagrams on Figure 9c and 9d (Kurt Hollocher *et al.*, 2012) show that rocks from the studied area are dominantly plotted as an alkaline arc with some samples plotted as a continental arc. Based on geochemical characteristic above, rocks in the thestudied area indicate that they were formed in a continental margin transitioning from subduction to late-subduction environment.

The rock samples used in this study have been weathered to different degrees. Thus, all of the data have high Loss on Ignition (LOI) values; the LOI values of the rock samples range from 2 – 10 wt. %, and the LOI values of the soil samples range from 13 – 21 wt. %. The geochemical analysis was carried out on the main and trace elements, considering trace elements had more immobile properties even though the rock had experienced weathering.

The CIA values in Tasipa Lava Unit range from 17.12 to 99.39. In the weathering rocks CIA values under 60 suggest lower weathering, 60–80 is moderate weathering, and more than 80 is extreme weathering samples from this unit. Thus plotted using A-CN-K ternary diagram (Figure 10a), the soil fell under extremely weathered and the plot gathered at Al_2O_3 peak, which could be linked to the presence of clay mineral in the soil (Nesbitt and Young, 1982; Fedo *et al.*, 1995). The IOL value ranges from 24.55 to 58.32. The progression from foidit rock to soil can be seen in Figure 10b, which depicts loss of Si and enrichment of Fe and Al during the lateritizion. Some of the soil was placed in kaolinitization stage, and some in weakly lateritization stage (Schellman, 1981; Babechuk *et al.*, 2014).

The SiO_2 content in the rock and soil in Tasipa Lava Unit is considerate low ranging between 28.59 to 57.29 wt. %, CaO ranges from 0.004 to 10.22 wt. %, Na_2O ranges from 0.00 to 9.42 wt. %, K_2O ranges from 0.03 to10.11 wt. %. These four show decrease from the rock to soil. Al_2O_3 ranges between 7.11 to 22.10 wt. %, and Fe_2O_3 ranges between 8.09 to 25.34 wt. %. They both increase from rock to soil. The decrease of silica, natrium, potassium, and calcium. The increase of aluminum contents from rock to soil display the formation of clay mineral from the weathering of feldspathoid, the high Fe_2O_3 content in the soil indicates that the clay formed could be Fe-rich clay or the soil is high in iron oxide minerals.

The total REE content in rock and soil in Tasipa Lava Unit ranges from 1077.80 to 7833.60 ppm, Th ranging between 204.30 to 883.60 ppm, and U ranging from 46.30 to 189.10 ppm. Th is enriched in weathering product, meanwhile U shows irregular trend (Figure 11a and 11b). Among REE

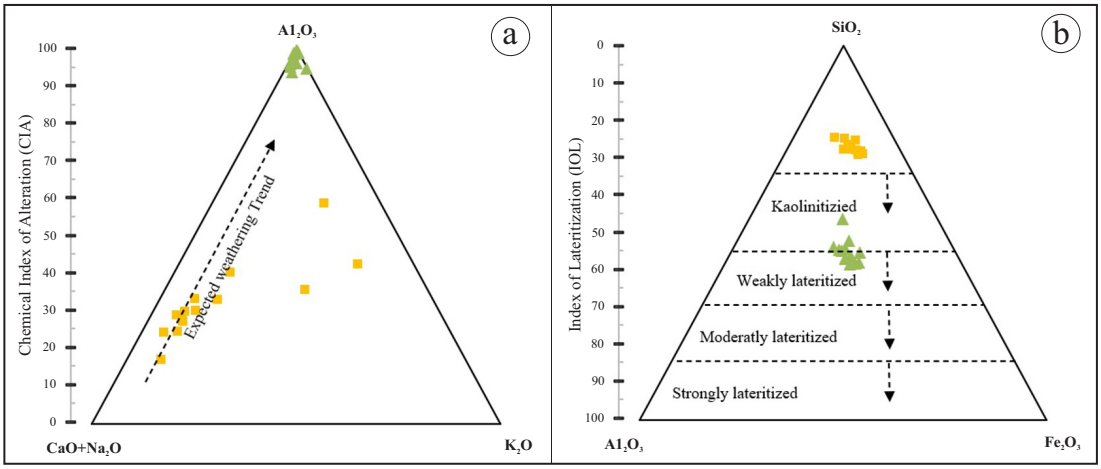

Figure 10. (a) A-CN-K ternary plots illustrating different degrees of alteration experienced in rocks and soil of Tasipa Lava Unit, the chemical index of alteration (CIA) is integrated into A-CN-K ternary plots; (b) SAF ternary plots illustrating the different degrees of alteration in rocks and soil of Tasipa Lava Unit, the index of lateritization (IOL) is integrated into SAF ternary diagram.

Figure 11. Selected element vs weathering indices: (a) U, (b) Th, (c) Total REE (TREE), and (d) Ce.

detected in these samples (Figure 11c), only Ce shows enrichment during weathering (Figure 11d), while the other shows irregular trends.

Radiometric Data Analysis

The variography analysis shows anisotropy in eU, eTh, and dose rate data in the NE–SW direction. For K data, however, it has not detected anisotropy as the range in all directions is the same. Hence, an omnidirectional experimental variogram was used for K data, while the other used a directional experimental variogram. The variogram was then modeled with a spherical and nested spherical variogram model. The variogram models are depicted in Table 2 with their corresponding variogram maps. The results are displayed in Figure 12, with an overlaying a geological map.

The radiometric maps of Rantedoda reveal how the structural features affected the distribu-

Table 2. Variogram Modes of Each Parameters And Their Corresponding Variogram Maps

Parameters	Model Type	Nugget Effect (C_0)	Sill (C)		Range (a)				Variogram maps
					a_1		a_2		
			C_1	C_2	Minor	Major	Minor	Major	
K	Nested Spherical	0.53	1.16	3.26	-	28	-	164	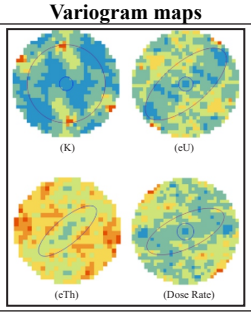
eU	Nested Spherical	30	350	50	-	50	150	350	
eTh	Spherical	2500	4450	-	330	950	-	-	
Dose rate	Nested Spherical	1000	60000	40000	-	40	80	200	

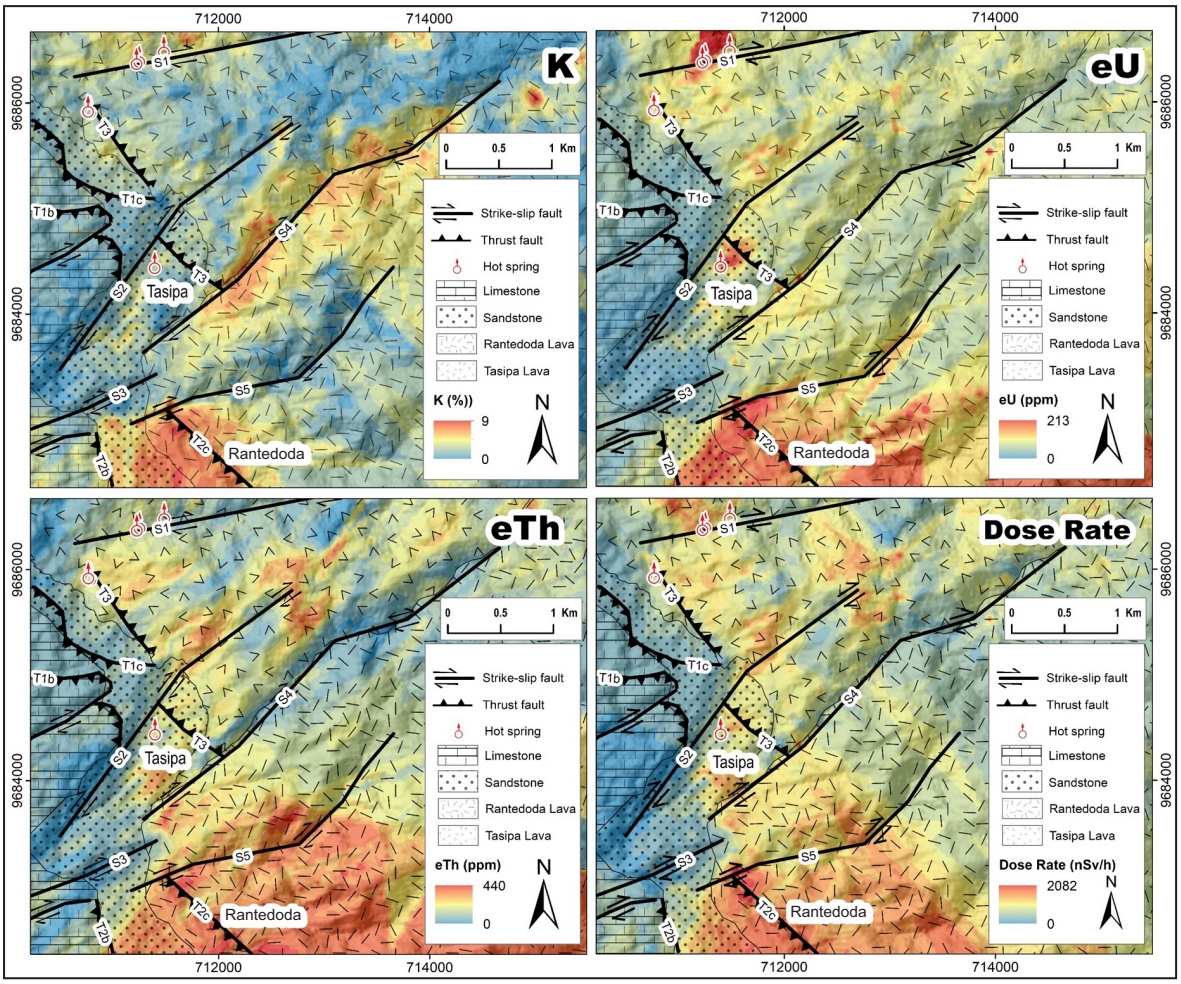

Figure 12. Kriging Result of each parameter with overlaying geological maps and structural features.

tion of K, eU, eTh, and dose rate values. It is also backed up by the anisotropic detected on the variogram maps of eU and eTh that follow the strike-slip faults trend of NE−SW. Meanwhile, the lithology does not comply with the radiometric map, except for the limestone unit, where all radiometric parameters show lower values. The high value of all radiometric parameters occurs in the southern part of the studied area near the T2c thrust fault. For K, the high radiometric value is limited near the T2c thrust fault, while for eU, eTh, and dose rate, the high radiometric value extends to the east. Moreover, the eU case follows the S5 strike-slip fault. The radiometric value trend that elongated along a fault was also observed in several locations. The K value is high along the

S4 strike slip-fault, while the opposite is observed in the eTh distribution. This phenomenon is also observed in the uphill of Tasipa region, between S1 and S4 fault. The eU, eTh, and dose rate values also seem bound to the T3 thrust fault, while there is only a slight increase in value for the K case. High values along the S1 strike-slip fault are seen on K and eU, whereas noncontinuous increasing values are detected in eTh and dose rate along the fault. The higher values of eU were also spotted near hot springs along the S1 strike-slip fault, and T3 thrust fault. This case has somehow faded on dose rate distribution, but the values are still high.

Discussion

The results of Rantedoda and Tasipa Lava Groups are similar to other volcanic rocks found in the Mamuju area. Volcanic rocks from Tapalang, Ampalas, Malunda, and Adang Complexes show the same magma series ranging from calc-alkaline to shoshonitic series, formed in subduction-related settings, with magma formation strongly influenced by the continental crust (Sukadana *et al.*, 2015; Draniswari *et al.*, 2020).

The geomorphic analysis, supported by ground checking of structural features, indicates that MSTM strongly contributed to the deformation of the studied area. The anisotropic distribution of radiometric parameters in NE-SW and NW -SE directions align with the fault trends, confirming structural control. Faults add a weak plane to the earth's surface, facilitating water movement. The interaction between water and rock below the surface may alter the composition, leading to the alteration and exogenic processes such as weathering and erosion. This is what happened to the volcanic rocks of Rantedoda. The deformation affected the radiometric distribution, but it is not the only factor controlling the U, Th, and REE enrichment, as weathering also plays a role.

The geochemical behaviours of K, U, and Th in soils are governed by complex interactions involving mineralogy and environmental conditions. The U is relatively more mobile than Th and K. Under oxidizing conditions, U is more soluble and mobile, contributing to its redistribution in soil profiles, and conversely, it will precipitate and become immobile in reducing conditions (Omel'yanenko *et al.*, 2007; Veerasamy *et al.*, 2020). On Rantedoda a high content of eU was noticed near the hot spring controlled by faults, such as the S1 strike-slip and T3 thrust faults. This suggests an outflow of subsurface water containing leached U from the volcanic rocks where faults become pathways, that further facilitate uranium transport into hot springs. Elevated U content from the leaching of surrounding rock where fault zones and weathering are heavily present is a common phenomenon, such as in U-rich black shales and granite in Okchun Belt, South Korea (Lee *et al.*, 1999), sandstone in Eastern Cape, South Africa (Madi *et al.*, 2014), metamorphites U deposit in Caldas Novas, Brazil (Lunardi and Bonotto, 2023), and uranium-rich volcanic rocks in Ardabil Province, Iran (Hadad and Doulatdar, 2008). These hot spring acidic and high-temperature conditions make them prime environments for uranium mobilization (Honda *et al.*, 1990).

Another phenomenon regarding radiometric response in Rantedoda is the inverse of K and eTh values in the northern part of the studied area. This may be caused by the behaviour of K and Th in the soil. Thorium exists almost exclusively as Th^{4+}, making it highly immobile under most environmental conditions. Its low solubility restricts its leaching and transport in soils, leading to accumulation in weathered horizons and residual soils (Buriánek *et al.*, 2022). Potassium is significantly more mobile than thorium, especially in soils with low cation-exchange capacity or sandy textures (Guagliardi *et al.*, 2020; Tzortzis and Tsertos, 2004). High Th values indicated enrichment due to weathering, where Th is left and other mobile elements, such as K and U, are leached. This is confirmed by geochemical analysis, which shows that Th and REE levels are higher in the soil than in the rock when plotted to the weathering indices (Figure 11). On the contrary, the high K with low Th values reflect relatively fresh rocks. This finding agrees with the slope angle map is depicted in Figure 13. Although almost all areas

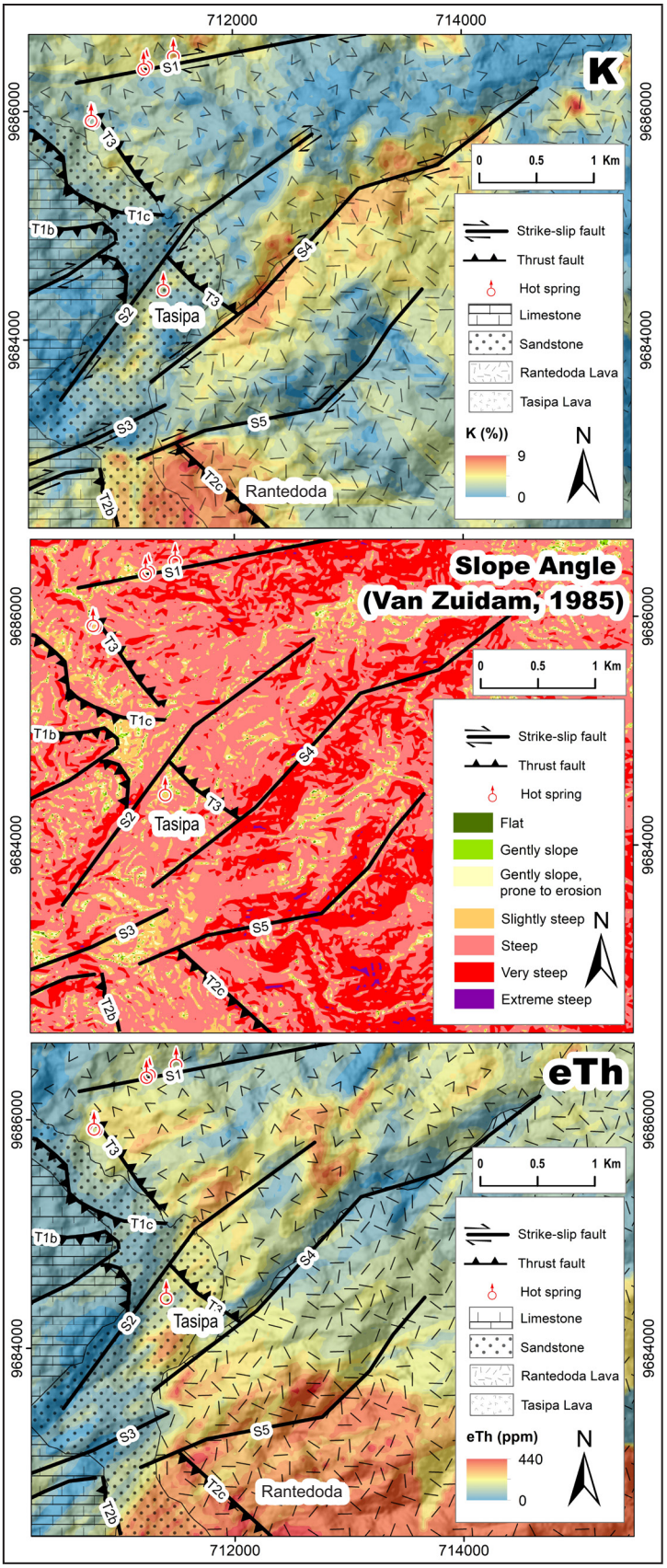

Figure 13. Comparison of K and eTh radiometric map with slope angle map from DEM (Slope angle classification adapted from Zuidam (1985).

of Rantedoda have steep slope angles, there is a difference in the area where high Th values lie in steep slope angles, and K is mostly high on very steep angles. Meteoric water tends to run off on the steeper slope, which coincides with the high K area, thus not accommodating further weathering. Meteoric water infiltrates the surface on a gentler slope, leading to rock weathering, thus enriching Th. Conversely, on this condition, K and other mobile elements stay on the rock as leaching is low. This suggests that direct faulting is not primary to control Th enrichment in the studied area, and weathering is more influential.

Micro-XRF study on Rantedoda demonstrated that the apatite and clay minerals, specifically montmorillonite and chlorite, which are present on the altered groundmass, are the sites of concentration for U and Th (Pratiwi *et al.*, 2024). This is the case for elevated K, eU, and surrounding the T2c Fault. Petrographic analysis confirms the presence of chlorite in RDD 1 and clay masses in RDD 1 and 5, which are the samples located near the area. K adsorption in clay minerals is a common and significant process in natural soils (Goli-Kalanpa *et al.*, 2008; Simonsson *et al.*, 2009; Li *et al.*, 2021). Many studies have explained U adsorption in alteration-product clay minerals, including kaolinite, montmorillonite, and smectite (Simonsson *et al.*, 2009; Campos *et al.*, 2013; Schindler *et al.*, 2015; Yang, 2023). The clay mineralogy influences U adsorption by providing specific pH conditions and ionic strength. On the granitic system, Th is immobile or has limited mobility during hydrothermal alteration like albitization and K-feldspathization (Leroy and Turpin, 1988; Abd El-Naby, 2009). Th is also found to be minimally mobilized in felsic volcanic rocks. Even under acidic conditions, its transport was negligible (Morales-Arredondo *et al.*, 2018). This finding suggests hydrothermal alteration of the Rantedoda volcanic rocks, which produced clay minerals, adsorb K and U while Th persists, leading to their enrichment, and may be facilitated by the T2c fault.

Based on these results, the exploration programme on U, Th, and REE on Rantedoda should address MSTM faults in the area. Faulting allows weathering that leads to Th and REE enrichment, controls leached U redistribution, and facilitates hydrothermal clay alteration that absorbs U. The radiometric method helped distinguish enriched alteration zones (high on all radiometric parameters) from the weathering zones (high on eTh, low on K) and resistant rock (high on K, low on eTh). Exploration programmes should intensively studied areas with clay alteration for potential secondary U, Th, and REE enrichment. While surface anomalies are valuable indicators, drilling programmes must confirm the vertical extent of mineralization in fault systems. Geophysical methods should be implemented to assist subsurface zones of hydrothermal activity identification. Weathered profiles near fault zones should be systematically sampled and analyzed for U, Th , and REE content. The findings in this study might not provide a comprehensive understanding across different geological settings other than the alkaline rocks of Adang Volcanics that are affected by MSTM as their geological setting provides sources and processes for U, Th, and REE enrichment. Nevertheless, the targeting strategy can be implemented for future U, Th, and REE prospection in other Mamuju areas.

Conclusions

The findings show that the MSTM fault system controls the mobilization and enrichment of U, Th, and REEs in the Rantedoda area. Faults are noted to create favourable conditions for mineralization. They make pathways for subsurface fluids, facilitate hydrothermal alteration, and influence weathering processes. Exploration programmes in Rantedoda should integrate structural analysis into geochemical, geological, and geophysical data to areas with clay alteration for potential secondary U, Th, and REE enrichment and weathered areas for lateritic Th and REE enrichment.

Acknowledgments

The authors extend sincere appreciation to the local communities of Tasipa and Rantedoda for their invaluable support and assistance during the fieldwork. Their contributions were instrumental in facilitating this research. The Authors also acknowledge Muhammad Wira Maulana, Faneza Nur Mardania, Sylviana Mulia, Adriel Sebastian, and Hera Agung Silaltopa for their efforts in sample preparation for petrographic and geochemical analyses. Furthermore, we express our gratitude to Sylviana Mulia, Alhayyu Druvadi Adnoor, and Mochamad Ikral Pamungkas for their assistance in processing the initial data. We also thank Rizky Firmansyah for the supplementary field documentation. Part of the scientific results in this work were obtained using Win-Tensor, a software developed by Dr. Damien Delvaux, Royal Museum for Central Africa, Tervuren, Belgium. The authors gratefully acknowledge the anonymous reviewer insightful comments and critical evaluations. Their thorough reviews and constructive feedback greatly contributed to this manuscript refinement and overall quality. This research was supported by the RP HITN 2024 Grant RO2-REA-C-006, awarded by the Research Organization of Nuclear Energy, National Research and Innovation Agency (BRIN).

Author Contribution

Conceptualization, Heri Syaeful, Roni Cahya Ciputra; methodology, Heri Syaeful, Roni Cahya Ciputra, I Gde Sukadana; formal analysis, Roni Cahya Ciputra, Fadiah Pratiwi, Aldo Febriansyah Putra, Tyto Baskara Adimedha; data acquisition, Heri Syaeful, Frederikus Dian Indrastomo, I Gde Sukadana; data curation, Yoshi Rachael, Frederikus Dian Indrastomo; writing-original draft preparation, Roni Cahya Ciputra, Fadiah Pratiwi, Aldo Febriansyah Putra, Yoshi Rachael; writing-review and editing, Heri Syaeful, I Gde Sukadana, Tyto Baskara Adimedha; visualization, Roni Cahya Ciputra, Fadiah Pratiwi, Aldo Febriansyah Putra; supervision, I Gde Sukadana, Frederikus Dian Indrastomo. All authors have read and agreed to the published version of the manuscript.

References

Abd El-Naby, H.H., 2009. High and low temperature alteration of uranium and thorium minerals, Um Ara granites, south Eastern Desert, Egypt. *Ore Geology Reviews*, Elsevier B.V., 35 (3-4), p.436-446. DOI: 10.1016/j.oregeorev.2009.02.006.

Babechuk, M.G., Widdowson, M., and Kamber, B.S., 2014. Quantifying chemical weathering intensity and trace element release from two contrasting basalt profiles, Deccan Traps, India, *Chemical Geology*, 363, January, p.56-75. DOI: 10.1016/j.chemgeo.2013.10.027.

Bachri, S. and Baharuddin, 2001. *Geological Map of the Majene-Malunda Quadrangle*, Scale 1 : 250.000. Geological Research and Development Centre, Bandung.

Buriánek, D., Ivanov, M., Janderková, J., and Patzel, M., 2022. Importance of accessory minerals for the vertical distribution of uranium and thorium in soil profiles: A case study of durbachite from the Třebíč Pluton (Czech Republic). *Catena*, 213, February. DOI: 10.1016/j.catena.2022.106166.

Calvert, S.J. and Hall, R., 2007. Cenozoic evolution of the Lariang and Karama regions, North Makassar Basin western Sulawesi, Indonesia. *Petroleum Geoscience*, 13 (4), p.353-368. DOI: 10.1144/1354-079306-757.

Campos, B., Aguilar-Carrillo, J., Algarra, M., Gonçalves, M.A., Rodríguez-Castellón, E., Esteves da Silva, J.C.G., and Bobos, I., 2013. Adsorption of uranyl ions on kaolinite, montmorillonite, humic acid and composite clay material. *Applied Clay Science*, Elsevier B.V., 85 (1), p.53-63. DOI: 10.1016/j.clay.2013.08.046.

Coffield, D.Q., Bergman, S.C., Garrard, R.A., Guritno, N., Robinson, N.M,. and Talbot, J., 1993.

Tectonic and Stratigraphic Evolution of the Kalosi PSC Area and Associated Development of a Tertiary Petroleum System, South Sulawesi, Indonesia. *Proceedings, Indonesian Petroleum Association Twenty-Second Annual Convention & Exhibition Indonesian Petroleum Association 22nd Annual Convention*, p.679-706.

Crippen, R., Buckley, S., Agram, P., Belz, E., Gurrola, E., Hensley, S., and Kobrick, M., 2016. Nasadem global elevation model: Methods and progress. *International Archives of the Photogrammetry, Remote Sensing and Spatial Information Sciences - ISPRS Archives*, *4, July*, p.125-128. DOI: 10.5194/isprsarchives-XLI-B4-125-2016.

Delvaux, D. and Sperner, B., 2003. Stress tensor inversion from fault kinematic indicators and focal mechanism data: the TENSOR program, In: Nieuwland, D. (ed.). *New Insights into Structural Interpretation and Modelling*, Geological Society, London, p.75-100.

Draniswari, W.A., Kusuma, S.I.T., Adimedha, T.B., and Sukadana, I.G., 2020. Peran Kontaminasi Kerak pada Diferensiasi Magma Pembentuk Batuan Vulkanik Sungai Ampalas, Mamuju, Sulawesi Barat. *Eksplorium*, 41 (2), p.73-86. DOI:10.17146/eksplorium.2020.41.2.6040.

Elburg, M., Leeuwen, T. van, Foden, J., and Muhardjo, 2003. Spatial and temporal isotopic domains of contrasting igneous suites in Western and Northern Sulawesi, Indonesia. *Chemical Geology*, 199 (3-4), p.243-276. DOI: 10.1016/S0009-2541(03)00084-6.

Fedo, C.M., Nesbitt, H.W., and Young, G.M., 1995. Unravelling the effects of potassium metamorphism in sedimentary rocks and paleosols, with implications for paleoweathering conditions and provenance. *Geology*, 23, p.921-924.

Goli-Kalanpa, E., Roozitalab, M.H., and Malakouti, M.J., 2008. Potassium availability as related to clay mineralogy and rates of potassium application. *Communications in Soil Science and Plant Analysis*, 39 (17-18), p.2721-2733. DOI: 10.1080/00103620802358870.

Guagliardi, I., Zuzolo, D., Albanese, S., Lima, A., Cerino, P., Pizzolante, A., and Thiombane, M., 2020. Uranium, thorium and potassium insights on Campania region (Italy) soils: Sources patterns based on compositional data analysis and fractal model. *Journal of Geochemical Exploration*, Elsevier, 212, February, p.106508. DOI:10.1016/j.gexplo.2020.106508.

Guntoro, A., 1999. The formation of the Makassar Strait and the separation between SE Kalimantan and SW Sulawesi. *Journal of Asian Earth Sciences*, 17 (1-2), p.79-98. DOI: 10.1016/S0743-9547(98)00037-3.

Hadad, K. and Doulatdar, R., 2008. U-series concentration in surface and ground water resources of Ardabil province. *Radiation Protection Dosimetry*, 130 (3), p.309-318. DOI: 10.1093/rpd/ncn001.

Hall, R. and Sevastjanova, I,. 2012. Australian crust in Indonesia. *Australian Journal of Earth Sciences*, 5 (6), p.827-844. DOI: 10.1080/08120099.2012.692335.

Hartiningsih, E., Syafrizal, Sucipta, I.G.B.E., Notosiswoyo, S., 2022. Multistage Gold Mineralization at The Wanagon Gold Prospect, Ertsberg District, Mimika Regency, Papua Province, Indonesia. *Indonesian Journal on Geoscience*, 9 (3), p.279-290. DOI: 10.17014/ijog.9.3.279-290

Hennig, J., Hall, R., and Armstrong, R.A., 2016. U-Pb zircon geochronology of rocks from west Central Sulawesi , Indonesia : Extension-related metamorphism and magmatism during the early stages of mountain building. *Gondwana Research*, International Association for Gondwana Research, 32, p.41-63. DOI: 10.1016/j.gr.2014.12.012.

Hennig, J., Hall, R., Forster, M.A., Kohn, B.P., and Lister, G.S., 2017. Rapid cooling and exhumation as a consequence of extension and crustal thinning: Inferences from the Late Miocene to Pliocene Palu Metamorphic Complex, Sulawesi, Indonesia. *Tectonophysics*, Elsevier B.V, 712-713, p.600-622. DOI: 10.1016/j.tecto.2017.06.025.

Honda, T., Oi, T., Ossaka, T., Nozaki, T., and Kakihana, H., 1990. Determination of thorium and uranium in hot spring and crater lake waters by neutron activation analysis. *Journal of Radioanalytical and Nuclear Chemistry Articles*, 139 (1), p.65-77. DOI: 10.1007/BF02060453.

Indrastomo, F.D., Sukadana, I.G., Saepuloh, A., Harsolumakso, A.H., and Kamajati, D., 2015. Interpretasi Vulkanostratigrafi Daerah Mamuju Berdasarkan Analisis Citra Landsat-8. *Eksplorium*, 36 (2), p.71-88. DOI: 10.17146/eksplorium.2015.36.2.2772.

Indrastomo, F.D., Sukadana, I.G., and Suharji, 2017. Identifikasi Pola Struktur Geologi Sebagai Pengontrol Sebaran Mineral Radioaktif Berdasarkan Kelurusan pada Citra Landsat-8 di Mamuju , Sulawesi Barat Identification of Geological Structure Pattern as Radioactive Minerals Distribution Control Based on Lan. *Eksplorium*, 38 (2), p.71-80.

Kanugrahan, S.P. and Hakam, D.F., 2023. Long-Term Scenarios of Indonesia Power Sector to Achieve Nationally Determined Contribution (NDC) 2060. *Energies*, 16 (12). DOI: 10.3390/en16124719.

Kurt Hollocher, Robinson, P., Walsh, E., and Roberts, D., 2012. Geochemistry of Amphibolite-facies Volcanics and Gabbros of The Støren Nappe in Extensions West and Southwest of Trondheim, Western Gneiss Region, Norway: a Key to Correlations and Paleotectonic Settings. *American Journalof Science*, 312 (4), p.357-416.

Lee, M.H., Kim, M.K., Shin, H.S., Choi, G.S., Hong, K.H., Cho, Y.H.. and Lee, C.W., 1999. Behavior of Uranium Isotopes in the Ground Water on the Okchun, *Proceedings of the Korean Nuclear Society Autumn Meeting*, p.328.1-328.9

Leeuwen, T.M. van and Muhardjo, 2005. Stratigraphy and tectonic setting of the Cretaceous and Paleogene volcanic-sedimentary successions in northwest Sulawesi, Indonesia: Implications for the Cenozoic evolution of Western and Northern Sulawesi. *Journal of Asian Earth Sciences*, 25 (3), p.481-511. DOI: 10.1016/j.jseaes.2004.05.004.

Leroy, J.L. and Turpin, L., 1988. REE, Th and U behaviour during hydrothermal and supergene processes in a granitic environment. *Chemical Geology*, 68 (3-4), p.239-251. DOI: 10.1016/0009-2541(88)90024-1.

Li, W., Liu, X.M., Hu, Y., Teng, F.Z., and Hu, Y., 2021. Potassium isotopic fractionation during clay adsorption. *Geochimica et Cosmochimica Acta*, Elsevier Ltd, 304, p.160-177. DOI: 10.1016/j.gca.2021.04.027.

Lunardi, M. and Bonotto, D.M., 2023. Natural radioactivity due to uranium and radon in thermal groundwaters of Central Brazil. *Journal of Radioanalytical and Nuclear Chemistry*, Springer International Publishing, 332 (3), p.629-646. DOI: 10.1007/s10967-023-08784-w.

Madi, K., Nyabeze, P., Gwavava, O., Sekiba, M., and Zhao, B., 2014. Uranium, thorium and potassium occurrences in the vicinity of hot springs in the northern neotectonic belt in the Eastern Cape Province, South Africa. *Journal of Radioanalytical and Nuclear Chemistry*, 301 (2), p.351-363. DOI: 10.1007/s10967-014-3183-1.

Maulana, A., Imai, A., Leeuwen, T. van, Watanabe, K., Yonezu, K., Nakano, T., Boyce, A., 2016. Origin and geodynamic setting of Late Cenozoic granitoids in Sulawesi, Indonesia. *Journal of Asian Earth Sciences*, Elsevier Ltd, 124, p.102-125. DOI: 10.1016/j.jseaes.2016.04.018.

Meilano, I., Salman, R., Susilo, S., Shiddiqi, H.A., Supendi, P., Lythgoe, K., and Tay, C., 2023. The 2021 M W 6.2 Mamuju, West Sulawesi, Indonesia earthquake: partial rupture of the Makassar Strait thrust. *Geophysical Journal International*, 233 (3), p.1694-1707. DOI: 10.1093/gji/ggac512.

Morales-Arredondo, J.I., Hernández, M.A.A., Hernández-Mendiola, E., Estrada-Hernández, R.E., and Bermea, O.M., 2018. Hydrogeochemical behavior of uranium and thorium in rock and groundwater samples from south-

eastern of El Bajío Guanajuatese, Guanajuato, Mexico. *Environmental Earth Sciences*, Springer Berlin Heidelberg, 77 (16), p.1-13. DOI: 10.1007/s12665-018-7749-z.

Moss, S.J. and Chambers, J.L.C., 1999. Tertiary facies architecture in the Kutai Basin, Kalimantan, Indonesia, *Journal of Asian Earth Sciences*, 17 (1-2), p.157-181, DOI: 10.1016/S0743-9547(98)00035-X.

Mu'awanah, F.R., Priadi, B., Widodo, W., Sukadana, I.G., and Andriansyah, R., 2019. Mobilitas Uranium pada Endapan Sedimen Sungai Aktif di Daerah Mamuju, Sulawesi Barat. *Eksplorium*, 39 (2), p.95-104. DOI: 10.17146/eksplorium.2018.39.2.4953.

Nesbitt, H.W. and Young, G.M., 1982. Early Proterozoic climates and plate motions inferred from major elements chemistry of lutites. *Nature*, 299 (5885), p.715-717.

Odigo, V. and Sambo, G.N., 2023. Geochemical Provenance, Source Area Weathering, and Tectonic Setting of the Bida Sandstone in the Northern Bida Basin, Northcentral Nigeria. *Indonesian Journal on Geoscience*, 10 (1), p.27-35. DOI: 10.17014/ijog.10.1.27-35

Omel'yanenko, B.I., Petrov, V.A., and Poluektov, V.V., 2007. Behavior of uranium under conditions of interaction of rocks and ores with subsurface water. *Geology of Ore Deposits*, 49 (5), p.378-391. DOI: 10.1134/S1075701507050042.

Pearce, J.A. and Cann, J.R., 1973. Tectonic setting of basic volcanic rocks determined using trace element analyses. *Earth and Planetary Science Letters*, 19 (2), p.290-300. DOI: 10.1016/0012-821X(73)90129-5.

Pearce, J.A., 1983. Role of the Sub-Continental Lithosphere in Magma Genesis at Active Continental Margins. *In*: Hawkesworth, C.J. and Norry, M.J. (eds.), and Mantle Xenoliths, Shiva Cheshire, p.230-249.

Peccerillo, A. and Taylor, S.R., 1976, Geochemistry of Eocene Calc-alkaline Volcanic Rocks from the Kastamonu Area, Northern Turkey. *Contributions to Mineralogy and Petrology*, 58 (1), p.63-81. DOI: 10.1007/BF00384745.

Permana, S., Trianti, N. and Rahmansyah, A., 2022. Nuclear Energy Contribution for Net Zero Emission and National Energy Mix 2060 in Indonesia. *Journal of Physics: Conference Series*, 2243 (012066) p.1-16. DOI: 10.1088/1742-6596/2243/1/012066.

Polvé, M., Maury, R.C., Bellon, H., Rangin, C., Priadi, B., Yuwono, S., and Joron, J.L., 1997. Magmatic evolution of Sulawesi (Indonesia): Constraints on the Cenozoic geodynamic history of the Sundaland active margin. *Tectonophysics*, 272 (1), p.69-92. DOI: 10.1016/S0040-1951(96)00276-4.

Pratiwi, F., Rachael, Y., Syaeful, H., Sukadana, I.G., and Indrastomo, F.D., 2024. Elemental Mapping Micro-XRF (EMMX) Analysis for Identifying Uranium and Thorium Bearing Minerals in Rantedoda Area, Mamuju, West Sulawesi. *AIP Conference Proceedings*, 2967 (70004), p.1-9. DOI: 10.1063/5.0192902.

Puspita, S.D., Robert, H., and Elders, C.F., 2005. Structural styles of the offshore West Sulawesi fold belt, North Makassar straits, Indonesia. *Proceedings, Indonesian Petroleum Association Thirtieth Annual Convention & Exhibition*, p.519-542. DOI: 10.29118/ipa.1002.05.g.110.

Raharjo, S., Seago, R., Jatmiko, E.W., Hakim, F.B., and Meckel, L.D., 2012. Basin Evolution and Hydrocarbon Geochemistry of The Lariang-Karama Basin: Implications For Petroleum System in Onshore West Sulawesi. *Proceedings, Indonesian Petroleum Association Thirty-Sixth Annual Convention & Exhibition*. DOI: 10.29118/ipa.0.12.g.135.

Rahmanta, M.A., Adhi, A.C., Tambunan, H.B., Digwijaya, W., Damanik, N., and Al Hasibi, R.A., 2023. An Analysis of National Position, Opportunity, and Challenge of Indonesia's Nuclear Program to Support Net-Zero Emissions by 2060. *Energies*, 16 (8089), p.1-37. DOI: 10.3390/en16248089.

Ratman, N. and Atmawinata, S., 1993. *Geological Map of The Mamuju Quadrangle*, Bandung.

Ritonga, R., Maulana, A., and Tonggiroh, A., 2021. Rare Earth Elements Distribution in

Weathered Volcanic Rock from Mamuju Area, West Sulawesi. *IOP Conference Series: Earth and Environmental Science*. 921 (012039), p.1-8. DOI: 10.1088/1755-1315/921/1/012039.

Rosianna, I., Nugraha, E.D., Syaeful, H., Putra, S., Hosoda, M., Akata, N., and Tokonami, S. 2020. Natural radioactivity of laterite and volcanic rock sample for radioactive mineral exploration in mamuju, indonesia. *Geosciences (Switzerland)*, 10 (9), p.1-13. DOI: 10.3390/geosciences10090376.

Rosianna, I., Nugraha, E.D., Tazoe, H., Syaeful, H., Muhammad, A.G., Sukadana, I.G., and Indrastomo, F.D., 2023. Uranium Isotope Characterization in Volcanic Deposits in a High Natural Background Radiation Area, Mamuju, Indonesia. *Geosciences (Switzerland)*, 13, (12), p.1-13. DOI: 10.3390/geosciences13120388.

Schellman, W., 1981. Consideration on the definition and classification of laterites. *Proceedings of the International Seminar on Lateritisation Processes*. Trivandrum, India. A.A. Balkema, Rotterdam, p.1-10.

Schindler, M., Legrand, C.A., and Hochella, M.F., 2015. Alteration, adsorption and nucleation processes on clay-water interfaces: Mechanisms for the retention of uranium by altered clay surfaces on the nanometer scale. *Geochimica et Cosmochimica Acta*, Elsevier Ltd, 153, p.15-36. DOI: 10.1016/j.gca.2014.12.020.

Serhalawan, Y. and Chen, P.F., 2024. Seismotectonics of Sulawesi, Indonesia. *Tectonophysics*, Elsevier B.V., 883 (230366), p.1-16. DOI: 10.1016/j.tecto.2024.230366.

Shah, K.U., Raghoo, P., and Blechinger, P., 2024. Is there a case for a coal moratorium in Indonesia? Power sector optimization modeling of low-carbon strategies. *Renewable and Sustainable Energy Transition*, Elsevier Ltd., 5 (100074), p.1-14. DOI: 10.1016/j.rset.2023.100074.

Simandjuntak, 1986. *Sedimentology and Tectonics Of The Collision Complex In The East Arm of Sulawesi*. University of London.

Simonsson, M., Hillier, S., and Öborn, I., 2009. Changes in clay minerals and potassium fixation capacity as a result of release and fixation of potassium in long-term field experiments. *Geoderma*, Elsevier B.V., 151 (3-4), p.109-120. DOI: 10.1016/j.geoderma.2009.03.018.

Sukadana, I.G., Harijoko, A., and Setijadji, L.D., 2015. Tataan Tektonika Batuan Gunung Api di Komplek Adang, Kabupaten Mamuju, Provinsi Sulawesi Barat. *Eksplorium*, 36 (1), p.31-44.

Sukadana, I.G., Syaeful, H., Indrastomo, F.D., Widana, K.S., and Rakhma, E. 2016, Identification of Mineralization Type and Specific Radioactive Minerals in Mamuju, West Sulawesi. *Journal of East China University of Technology,* 39, p.39-44.

Sukadana, I.G., Warmada, I.W., Harijoko, A., Indrastomo, F.D., and Syaeful, H., 2021. The Application of Geostatistical Analysis on Radiometric Mapping Data to Recognized the Uranium and Thorium Anomaly in West Sulawesi, Indonesia. *IOP Conference Series: Earth and Environmental Science*, 819 (1). DOI: 10.1088/1755-1315/819/1/012030.

Sukadana, I.G., Warmada, I.W., Pratiwi, F., Harijoko, A., and Adimedha, T.B., 2022. Elemental Mapping for Characterizing of Thorium and Rare Earth Elements (REE) Bearing Minerals Using μXRF. *Atom Indonesia*, 48 (2), p.87-98.

Sukadana, I.G., 2023. *Magma Evolution and Radioactive Minerals Enrichment in Adang Volcanic Rocks in Mamuju, West Sulawesi.*, Universitas Gadjah Mada, Sleman, Indonesia.

Syaeful, H., Sukadana, I.G., and Sumaryanto, A., 2014. Radiometric Mapping for Naturally Occurring Radioactive Materials (NORM) Assessment in Mamuju, West Sulawesi.*Atom Indonesia*, 40 (1), p.33-39. DOI: 10.17146/aij.2014.263.

Syaeful, H., Sukadana, I.G., Indrastomo, F.D., Muhammad, A.G.. and Ngadenin, 2021. Uranium Exploration, Deposit and Resources: The Key of Nuclear Power Plant Development Program in Indonesia Uranium Exploration ,

Deposit and Resources: The Key of Nuclear Power Plant Development Program in Indonesia. *Journal of Physics: Conference Series*, 2048 (012003), p.1-9. DOI: 10.1088/1742-6596/2048/1/012003.

Syaeful, H., Muhammad, A.G., Rachael, Y., Pratiwi, F., Rosianna, I., Ngadenin, N., and Indrastomo, F.D., 2024. Delineation of permissive tract for 3-part quantitative undiscovered resources assessment of uranium and thorium in Mamuju, West Sulawesi. *AIP Conference Proceedings*, 2967 (110013), p.1-9.

Tzortzis, M. and Tsertos, H., 2004. Determination of thorium, uranium and potassium elemental concentrations in surface soils in Cyprus. *Journal of Environmental Radioactivity*, 77 (3), p.325-338. DOI: 10.1016/j.jenvrad.2004.03.014.

Veerasamy, N., Sahoo, S.K., Inoue, K., Arae, H., and Fukushi, M., 2020. Geochemical behavior of uranium and thorium in sand and sandy soil samples from a natural high background radiation area of the Odisha coast, India. *Environmental Science and Pollution Research*, 27 (25), p.31339-31349. DOI: 10.1007/s11356-020-09370-3.

Winarno, T., Ali, R. K., Simangunsong, H., and Almiftahurrizqi, 2023. Characteristics and Genesis of Laterite Bauxite in Sompak District and Surrounding Areas, Landak Regency, West Kalimantan. *Indonesian Journal on Geoscience*, 10 (1), p.37-49. DOI: 10.17014/ijog.10.1.37-49

Winchester, J.A. and Floyd, P.A., 1977. Geochemical discrimination of different magma series and their differentiation products using immobile elements. *Chemical Geology*, *20*.

Winter, J.D., 2014. *Principles of Igneous and Metamorphic Petrology*, *Second*, Pearson Education Limited.

Wood, D.A., 1980. The Application of A Th-Hf-Ta Diagram to Problems of Tectonomagmatic Classification to Establishing The Nature Of Crustal CONTAMINATION OF BASALTIC LAVAS OF THE BRITISH TERTIARY VOLCANIC PROVINCE. *Earth and Planetary Science Letters*, 50, p.11-30.

Yang, G., 2023. Sorption and reduction of hexavalent uranium by natural and modified silicate minerals: A review. *Environmental Chemistry Letters*, Springer International Publishing, 21 (4), p.2441-2470. DOI: 10.1007/s10311-023-01606-1.

Zuidam, R.A. van, 1985. *Aerial Photo-Interpretation in Terrain Analysis and Geomorphologic Mapping*, Smits Publishers, Netherland.